Update of inter-comparison of HONO profiles derived from MAX-DOAS observations during the CINDI-2 campaign

Yang Wang (1) (Email: y.wang@mpic.de), S. Donner (1), T. Wagner (1), F. Hendrick (2), M. Van Roozendael (2), M. M. Friedrich (2), J. L. Tirpitz (3), U. Frieß (3), J. Lampel (3), S. Schmitt (3), A. S. López (4), N. Benavent (4), D. Garcia (4), J. Jin (5), J. Z. Ma (6), A. Piters (7), A. Apituley (7), B. Henzing (8), A. Bais (9), T. Drosoglou (9), Z. R. Wang (10), O. Postylyakov (11), A. Borovski (11), R. Querel (12), L. Gómez (13), I. Bruchkouski (14), C. Liu (15), H. R. Liu (15), C. Z. Xing (15), C. X. Zhang (15), K. Kreher (16), R. M. Volkamer (17), H. Finkenzeller (17), T. Koenig (17), P. H. Xie (18), J. Xu (18), X. Tian (18), O. L. Polyansky (19, 20), L. Lodi (20), A. Hilboll (21), K. L. CHAN (22)

MAX PLANCK INSTITUTE FOR CHEMISTRY

(1) Max Planck Institute for Chemistry, Mainz, Germany. (2) Belgian Institute for Space Aeronomy – BIRA-IASB, Brussels, Belgium. (3) Institute of Environmental Physics, University of Heidelberg, Heidelberg, Germany. (4) Department of Atmospheric Chemistry and Climate, Instituto de Química Física Rocasolano-CSIC, Madrid, Spain. (5) CMA Meteorological Observation Centre, Beijing, China
(6) Chinese Academy of Meteorological Sciences, Beijing, China. (7) Koninklijk Nederlands Meteorologisch Instituut, De Bilt, The Netherlands. (8) Netherlands Organisation for Applied Scientific Research (TNO), Utrecht, the Netherland. (9) Laboratory of Atmospheric Physics, Aristotle University of Thessaloniki, Thessaloniki, Greece. (10) Remote Sensing Technology Institute, German Aerospace Center (DLR), Oberpfaffenhofen, Germany. (11) A.M.Obukhov Institute of Atmospheric Physics, Russian Academy of Sciences, Moscow, Russia. (12) National Institute of Water & Atmospheric Research (NIWA), Lauder, New Zealand. (13) Area de Investigación e Instrumentación Atmosférica, INTA, Torrejón de Ardoz, Spain. (14) National Ozone Monitoring Research and Education Center BSU (NOMREC BSU), Belarusian State University (BSU), Minsk, Belarus. (15) School of Earth and Space Sciences, University of Science and Technology of China (USTC), Hefei, China. (16) BK Scientific GmbH, Mainz, Germany. (17) Department of Chemistry and Biochemistry, University of Colorado, Boulder, CO, USA. (18) Anhui Institute of Optics and Fine Mechanics, Key laboratory of Environmental Optics and Technology, Chinese Academy of Sciences, Hefei, China. (19) Institute of Applied Physics, Russian Academy of Sciences, Nizhny Novgorod, Russia. (20) Department of Physics and Astronomy, University College London, Gower St, London WC1E 6BT, UK. (21) Institute of Environmental Physics, University of Bremen, Bremen, Germany. (22) Meteorological Institute, Ludwig-Maximilians Universität München, Munich, Germany.

1. Abstract

In this poster, we update the comparison results of the HONO vertical profile retrievals during the CINDI-2 campaign.

2. comparison of HONO profiles from different instruments and algorithms

HONO profiles retrieved from different instruments and using different retrieval algorithms are compared. The activities are individually done for four tasks to constrain the uncertainties due to instruments, algorithms, aerosols, and FRS used for HONO dSCD fits. The four tasks and corresponding participants are described in Tabel 1. The comparison results between different participants are shown in Fig. 1. The comparisons of the retrieved near-surface results with the co-located LP-DOAS measurements are shown in Fig. 2. The comparisons of the retrieved HONO results between the HONO dSCDs retrieved with the sequential FRS (T1a) and the daily noon FRS (T1b) are shown in Fig. 3.

Table 1. Tasks and participants of profile comparison

Tasks	Description	Participants (algorithm)
T1a	retrieved from HONO dSCDs with the sequential FRS from individual instruments.	MPIC (PriAM), BIRA (BePro), CMA (PriAM), AIOFM (PriAM), USTC (HePro)
T1b	retrieved from HONO dSCDs with the daily FRS from individual instruments.	MPIC (PriAM), BIRA (BePro), CMA (PriAM), AIOFM (PriAM), USTC (HePro)
T2a	retrieved from common HONO dSCDs with common aerosol input	MPIC (PriAM), BIRA (BePro), BIRA_MMF(MMF), AUTH(BePro), USTC (HePro)
T2b	retrieved from common HONO dSCDs with aerosols individually retrieved from common O_4 dSCDs	MPIC (PriAM), BIRA (BePro), BIRA_MMF(MMF), AUTH(BePro), USTC (HePro)

Fig. 1 comparisons of results of the four tasks (different columns): (1) overview of HONO profiles in sampled days; (2) scatter plots and linear regressions of modeled and measured HONO dSCDs; (3) scatter plots and linear regressions of retrieved HONO number densities and median values at three altitudes; (4) histograms of differences of retrieved and median values at three altitudes; average and standard deviations are given in the brackets.

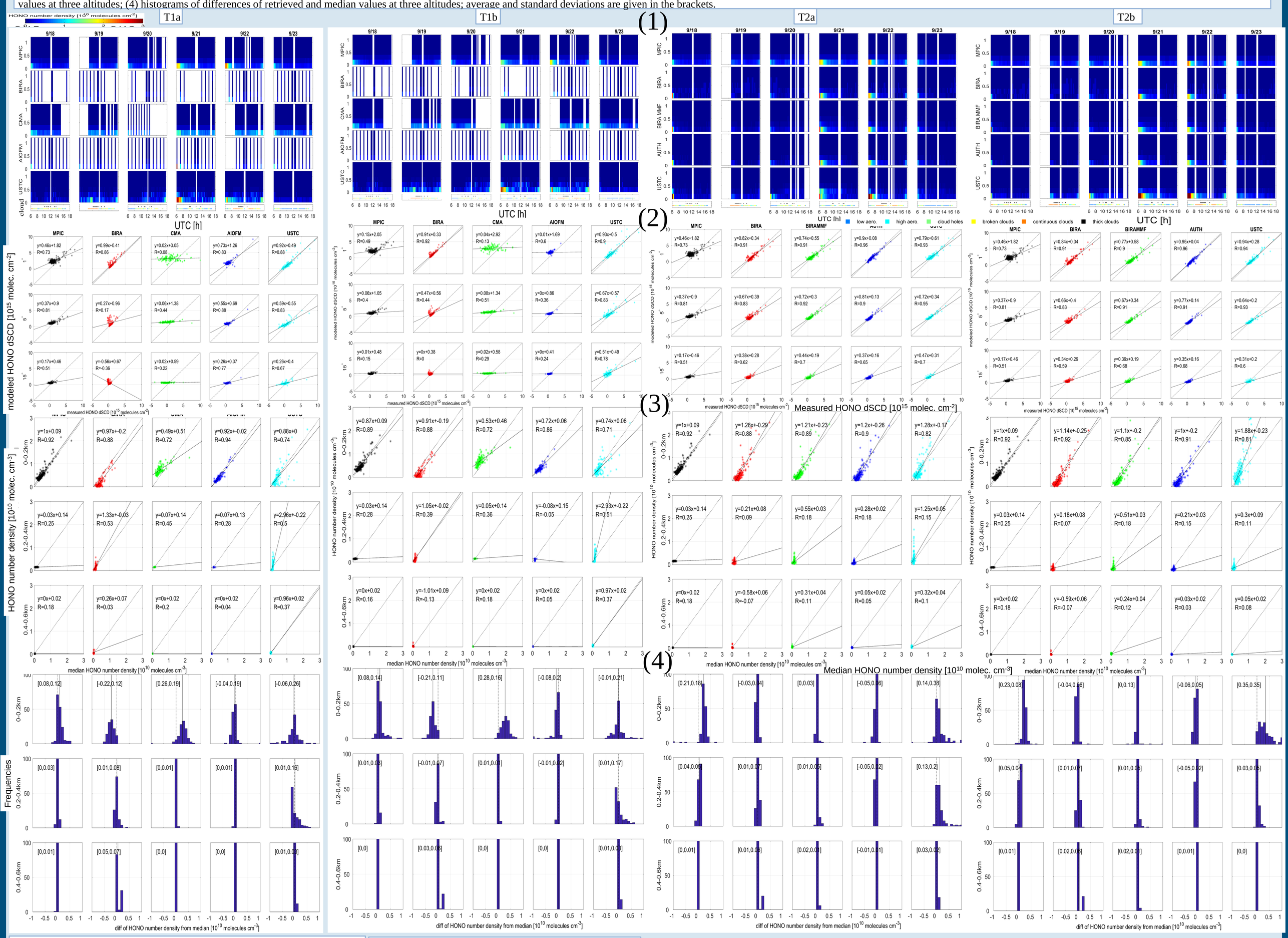

Fig. 2 for the four tasks (different rows) and different participants (different columns), retrieved near-surface HONO number densities compared between MAX-DOAS and LP-DOAS measurement

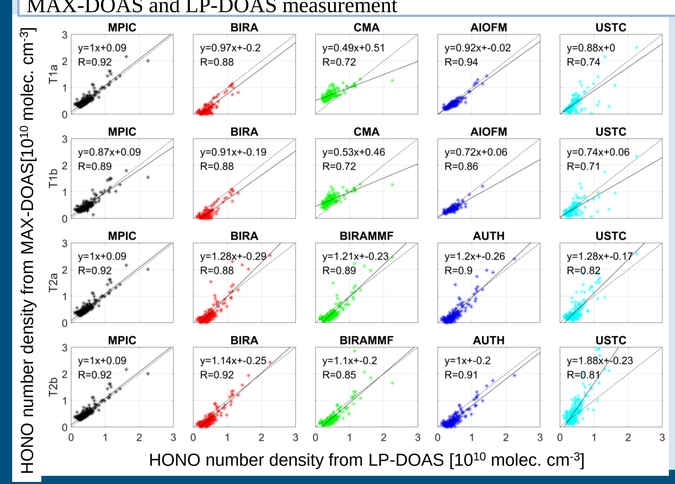

Fig. 3 median values, scatter plots and linear regressions of retrieved near-surface HONO number densities between retrievals using the daily FRS (T1b) and the sequential FRS (T1a)

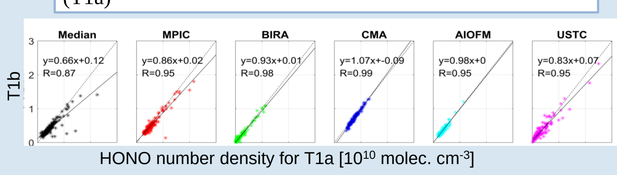

3. Summary:

The best agreement of modeled and measured HONO dSCDs is found for AUTH and USTC. The best agreement of retrieved HONO profiles between the different participants are found for the T2a task (the common HONO dSCD and and aerosols). Larger systematic deviations, especially for USTC, are found for the T2b (self-retrieved aerosols) compared to T2a. Larger scatter is found for the T1a and T1b tasks compared to T2a and T2b tasks due to different instruments. For the comparisons of retrieved near-surface HONO with LP-DOAS results: (1) for T2a, good agreements are found for all participants; (2) for T2b, only larger deviations are found for USTC; (3) for T1a and T1b, larger scatter is found for CMA and USTC. For the comparisons of retrieved HONO between T1a and T1b (different FRS) for individual instruments: larger deviations are found for MPIC and USTC.